Microstructure of Al-Zn and Zn-Al Alloys

Skoko, Željko; Popović, Stanko; Štefančić, Goran

CROATICA CHEMICA ACTA
CCACAA, ISSN-0011-1643, ISSN-1334-417X

Croat. Chem. Acta **82** (2) (2009) 405–420
CCA-3330

Original Scientific Paper

Microstructure of Al-Zn and Zn-Al Alloys*

Željko Skoko,[a] Stanko Popović,[a,] and Goran Štefanić[b]**

[a]*Physics Department, Faculty of Science, University of Zagreb, P. O. Box 331, 10002 Zagreb, Croatia*
[b]*Ruđer Bošković Institute, P. O. Box 180, 10002 Zagreb, Croatia*

RECEIVED APRIL 24, 2008; REVISED DECEMBER 8, 2008; ACCEPTED DECEMBER 9, 2008

Abstract. The change of microstructure of the title alloys with concentration, temperature and applied thermal treatment was studied *in situ* by XRD. The alloys, having the Zn atomic fraction, x(Zn), from 0.03 to 0.62, were subjected to: (i) rapid quenching from a temperature, T_t, higher than the solid-solution temperature, T_{ss}, in water at RT (samples WQ); (ii) slow cooling from T_t to RT (samples SC). The WQ's were solid solutions immediately after quenching, up to x(Zn) ≤ 0.44. For short ageing time, the WQ's contained GP zones, rich in Zn; by a prolonged ageing the WQ's were transformed to a quasi-equilibrium state, containing β precipitates, very rich in Zn. The SC's, also containing β precipitates, were closer to the equilibrium state than the aged WQ's, the microstructure of the latter depended on residual strains, quenched-in vacancies and a non-uniform distribution of β precipitates. Both SC's and prolongedly aged WQ's were slowly heated from RT to T_t and cooled back to RT. Several phenomena were observed in the heating run: a decrease of diffraction line intensities due to enhanced atom vibrations, anisotropy of thermal expansion, change in the precipitate shape, partial or complete dissolution of precipitates, phase transitions, formation of solid solution. In the cooling run, the alloys exhibited a temperature hysteresis in reversal phase transitions. The temperature dependence of microstructure for the SC's was different from that of prolongedly aged WQ's. The sequence of phase transitions, found for the alloys with x(Zn) ≥ 0.44, was not in line with the phase diagram of the Al-Zn system, accepted in literature.

Keywords: Al-Zn alloy, solid solution, precipitation in solid, phase transition, X-ray powder diffraction, differential scanning calorimetry

INTRODUCTION

Alloys are intermetallic phases or solid solutions and, as in the case of pure metals, in most cases can be regarded as close-packed structures. Solid solutions are very common in crystalline materials. A solid solution is basically a crystalline phase that can have variable composition; it may be interstitial or substitutional, or have a more complex structure.[1]

The system Al-Zn is very suitable and particularly attractive for studying microstructure and phase transitions, especially in the supersaturated state, with respect to the composition and applied thermal treatment. It has been studied by many authors, who have applied very different experimental methods as well as theoretical considerations in order to explain observed phenomena. Most of the collected knowledge can be found in a recent comprehensive monographs edited by H. Löffler, containing about 700 references.[2]

The solubility of Zn in Al is the largest among all elements, showing a maximum of 67(1) at% (mole fraction of Zn×100) at 654(2) K.[2,3] This is obviously due to the fact that Zn and Al do not form intermetallic phases or, in other words, the interaction between Al and Zn atoms is fairly weak. At room temperature, RT (298 K), the solubility of Zn in Al amounts 0.85 at%, and the one of Al in Zn is smaller than 0.5 at%.[2,3] The atomic radius of Al is 0.143 nm, while the one of Zn is 0.134 nm, this difference of approximately 7 % having a great influence on the microstructure of the Al-Zn and Zn-Al alloys.

Al-Zn or Zn-Al alloys can gradually (asymptotically) approach the equilibrium state after, for instance, rapid quenching and a prolonged ageing at, say, RT. That process can be accelerated at an elevated temperature, say, several tens K's above RT. In such a state, the alloy contains two phases: α-phase (fcc, the matrix, M) containing ≈ 99 at% Al and ≈ 1 at% Zn, and β-phase

* Dedicated to Professor Emeritus Drago Grdenić, Fellow of the Croatian Academy of Sciences and Arts, on the occasion of his 90th birthday.

** Author to whom correspondence should be addressed. (E-mail: spopovic@phy.hr)

(hexagonal, the precipitates), often denoted in literature as β(Zn), having ≈ 99.5 at% Zn and ≈ 0.5 at% Al.[2,3] It is said that the phase α(M/β) is in equilibrium with the phase β.

As the solubility of Zn in Al increases with temperature, the solid solution is formed at a certain temperature, T_{ss}. For instance, T_{ss} = 625 K for the alloy having the Zn atomic fraction, x(Zn) of 0.395.[2,4] After homogenization of the solid solution at a temperature, T_t, higher than T_{ss}, and rapid quenching to RT, the alloy is a supersaturated solid solution at RT. The decomposition of such unstable alloy takes place immediately after quenching, in nucleation and growth of spherical Guinier-Preston zones (GPZ), containing ≈ 70 at% Zn.[2,3] Diffusion of Zn atoms through the Al lattice, essential in formation of GPZ, can be explained by the existence of quenched-in vacancies.[2] Therefore, the first decomposition state is a two-phase system, at least up to x(Zn) ≤ 0.44,[5,6] consisting of the α(M/GPZ)-phase (fcc) in a metastable equilibrium with a dense system of GPZ. During a prolonged ageing, at RT or at an elevated temperature, the decomposition proceeds in a sequence of precipitates, the longest one is as follows: spherical GPZ [fcc, having the diameter up to 3 to 4 nm and being fully coherent with the host phase, α(M/GPZ)] – ellipsoidal GPZ (fcc, fully coherent with the host phase) – rhombohedrally distorted α'_R-precipitates (partially coherent with the host phase, having about ten nanometers in size) – metastable α'-phase [fcc, rather rich in Zn and being partially coherent with the host phase, α(M/α)] – β-phase [the final equilibrium precipitates, having micrometer sizes and being incoherent with the host phase, α(M/β)]. That sequence of phase transitions from one to the next type of precipitates depends on the initial composition of the alloy and on the applied thermal treatment.[2] The interface energy is a rather large component of the total free nucleation energy during the formation of small clusters of β-phase. That results in a fairly long sequence of metastable phases in the decomposition of the supersaturated Al-Zn alloys. The gain of free energy associated with the formation of the equilibrium β-phase is reduced with increasing the ageing temperature, at which the alloy decomposes. That is, the sequence of intermediate phases shortens as the ageing temperature decreases. For ageing at RT, a direct transition of big GPZ's to β precipitates is to be expected.[2,5,6] The phase diagram of the system Al-Zn has been defined on the basis of a number of papers and accepted in the literature.[2,4] The ageing time necessary to approach the equilibrium state, in which the α(M/β)-phase, depleted in Zn, is in equilibrium with β precipitates, decreases with the increase of x(Zn) and the ageing temperature.

Although much experimental and theoretical evidence on the Al-Zn system has been published in papers and monographs (*e.g.*[2,3]), a necessity has appeared recently to undertake a systematic and accurate study of the system by X-ray powder diffraction, lacking in the literature. A series of Al-Zn alloys, having the Zn atomic fraction, x(Zn), in the interval from 0.03 to 0.62, were subjected to various thermal treatments. The alloys were quenched rapidly to RT from a temperature, T_t, higher than the solid-solution temperature, T_{ss}, and then aged at RT or at elevated temperature. During ageing, the precipitation processes taking place in decomposition of supersaturated solid solutions were followed in detail. Also, the quenched and aged alloys, as well as the alloys slowly cooled from T_t to RT, that had approached the equilibrium state, were subjected to a gradual change of temperature, from RT to T_t and back to RT, and the changes of their microstructure were studied *in situ* by XRD.[5–11] These XRD studies have shown how accurately aimed and performed experiments may yield useful information, for instance, on the Zn fraction solved/retained in the matrix, M, for different precipitates, P, on the strains occurring at the M/P interface, on the unit-cell parameters of the supersaturated solid solutions at RT, of the intermediate phase, α', at temperatures of its existence, of the solid solution at T_{ss}, and of the equilibrium phase, β. New data have been obtained on the anisotropy of thermal expansion of the β-phase, on the shape change of β precipitates during thermal treatment, on the temperature hysteresis in the β→α' / α'→β phase transition. Recent investigations have shown that a correction of the phase diagram is necessary.

The present paper is a concise review of the recent XRD studies of Al-Zn and Zn-Al alloys, as outlined above, which are discussed in connection with new unpublished results. The paper is mainly focused on the XRD study of the temperature dependence of microstructure of the alloys with a high Zn content, with the aim of checking the validity of the phase diagram in its middle part, where the fractions of Al and Zn are comparable.

EXPERIMENTAL

The alloys were produced from elements of purity 4N. After a homogenization treatment, thin foils were prepared by cold rolling with intermediate annealing. The Al-Zn and Zn-Al alloys with the following Zn atomic fraction, x(Zn), were studied: 0.03, 0.045, 0.08, 0.15, 0.20, 0.24, 0.26, 0.35, 0.38, 0.40, 0.44, 0.48, 0.54 and 0.62. The specimens for XRD were: foils thick about

0.15 mm; fine powders prepared by filing bulk alloys and having particles of the size from 10 to 50 μm; needles cut-off from the foils and having approximate size 10×0.20×0.15 mm^3. Foils showed a strong preferred orientation of crystal grains and seldom exhibited diffraction lines at highest Bragg angles of a sufficient and reproducible intensity. Therefore, it was decided to dominantly use fine powders for diffraction studies in order to have a random orientation of crystal grains.

Diffraction patterns of fine powders and foils were taken by a Philips diffractometer, having a high-temperature Anton Paar attachment, a proportional counter and a graphite monochromator, with Cu*K*α radiation. Diffraction patterns of needles were taken by a Debye-Scherrer camera and using Ni-filtered Cu*K*α radiation. That technique enabled to utilize the spectral doublet of the α-phase diffraction line 511+333 at the highest Bragg angle, $\theta > 81°$, in accurate unit-cell parameter measurement. Appropriate precautions were applied in minimization of systematic aberrations, which influence the positions of diffraction lines,[12] as well as in manipulation with specimens, especially with needles, in order to prevent any transfer of heat to them. During diffraction experiments *in situ* at high temperature, specimens were exposed either to the standard air pressure of 10^5 Pa, or to a low air pressure of 10^{-3} Pa, but no oxidation effect was observed by XRD.

The following thermal treatments were applied:

1) The alloys (specimens in the form of fine powders, foils, needles) were slowly heated in a "vertical" furnace from RT to a temperature, T_t, higher than the solid solution temperature, T_{ss}, and were held at T_t for two hours. Then, the specimens were quenched inside the furnace in water at RT. A 1 m long aluminium tube full of water was inserted into the furnace a second before the quench. The free-fall path of the specimen to the water surface was about 10 mm, and rapid quenching took place by letting the specimen fall through the long water column. These specimens were denoted as "water quenched", WQ. In these experiments fine powders were wrapped in a thin aluminium foil, perforated with many small holes made by a steel needle. That procedure preserved the powder during quenching and enhanced the quenching rate, which was estimated to 10^5 K/s. Several prominent diffraction lines of fine powders or foils were scanned within thirty minutes after quenching. Needles were fixed to a straight thin aluminium stick by a very fine copper wire; in such a way, the needles were not lost during quenching in the water column. Diffraction patterns of the quenched needles were taken in the Debye-Scherrer camera within three hours after quenching.

2) The specimens (fine powders, foils) were slowly heated from RT to T_t, held at T_t for two hours and then slowly cooled to RT within the furnace over two days. These specimens were denoted as "slowly cooled", SC.

3) The specimens (fine powders) that had been quenched from T_t to RT, were annealed at 520 K for five days, and then slowly cooled to RT within the furnace over fifteen days. These specimens were denoted as "water-quenched-annealed-slowly-cooled", WQASC.

4) The specimens (fine powders), that had been quenched from T_t to RT, were aged at RT or at elevated temperature (up to 350 K, in order to enhance the decomposition rate in alloys with small Zn fraction) for prolonged time intervals, up to 11 months. These specimens were denoted as "water-quenched-prolongedly aged", WQPA.

5) The specimens (fine powders) that had been quenched from T_t to RT and prolongedly aged at RT (WQPA), and the specimens (fine powders) that had been slowly heated from RT to T_t and slowly cooled to RT (SC), all of them having approached the equilibrium state and being two-phase systems, α(M/β)+β, were slowly heated from RT to T_t and then slowly cooled to RT inside the diffractometer. The heating and cooling of the specimens, with a rate of 2 to 3 K/min, was stopped at a series of temperatures for 15 minutes in order to scan prominent diffraction lines of the α-phase and precipitates. In some cases, two or three heating and cooling cycles, between RT and T_t, were performed with the same specimen in order to check for reproducibility of results. The specimen holder and (at the same time) the specimen heater was a platinum strip (in fact a platinum alloy). Diffraction lines of platinum helped to calibrate the angular scale of the diffractometer at high temperature, utilizing its thermal expansion coefficient, amounting $10(1)\times10^{-6}$ K, as measured by the same diffractometer.

The notation of the alloys, having similar Al and Zn atomic fractions, was as follows.

(i) The alloys having x(Zn) = 0.44 and 0.48:

- WQAA, water-quenched from T_t to RT and aged at RT for two weeks [x(Zn) = 0.44] or for one week [x(Zn) = 0.48], with Al as the major element;

- WQPAA, water-quenched from T_t to RT and prolongedly aged at RT for 11 months, with Al as the major element;
- SCA, slowly cooled from T_t to RT, with Al as the major element.

(ii) The alloys having x(Zn) = 0.54 and 0.62:

- WQPAZ, water-quenched from T_t to RT and prolongedly aged at RT for 11 months, with Zn as the major element.

For comparison, pure aluminium was quenched and slowly cooled from T_t to RT in the same way as the Al-Zn alloys.

In order to choose appropriate diffraction lines of the phases α and β one had to take in account the facts: α111 is partially overlapped with β100, α420 with β114, α422 with β006 (very weak) and β212. Out of three high Bragg angle diffraction lines of the α-phase, which can be followed by the counter diffractometer and are very helpful in accurate work, only α331 is free of β-phase diffraction lines. However, in as-quenched alloys, diffraction lines of the β-phase were not present, or were rather weak for high x(Zn) values, and all high-angle α-phase diffraction lines could be followed. Moreover, using the Debye-Scherrer technique, the diffraction line α511+333 at $\theta > 81°$ can be measured. On the other hand, an appropriate diffraction line of the β-phase at high Bragg angle, having a fair intensity and being free of the α-phase diffraction lines, is β211.

Thermal behavior of the Al-Zn alloy (fine powder) with x(Zn) = 0.24 was followed by differential scanning calorimetry (DSC): absorption of heat during the β→α' phase transition on heating and release of heat during the α'→β phase transition on cooling. The DSC analysis was performed up to 600 K with a scanning rate of 10 K min^{-1} using a Perkin-Elmer DSC, model 7. The instrument was connected to a personal computer loaded with a program for processing the obtained DSC curves. During the DSC measurements, extra pure nitrogen (N_2) was used as a purging gas. The sample mass was adjusted to ≈ 10 mg.

RESULTS AND DISCUSSION

Aluminium

The unit-cell parameter of pure Al, quenched from T_t to RT, was practically the same to that of Al, slowly cooled from T_t to RT, amounting a(Al) = 0.40494(1) nm (space group $Fm3m$) at RT (298 K). The quenched Al showed broader diffraction lines than did the slowly cooled Al, due to lattice defects introduced in the crystal lattice during quenching.

Microstructure of Slowly Cooled Alloys

The alloys slowly heated from RT to T_t and slowly cooled back to RT (specimens SC) were two-phase systems, containing α(M/β)- and β-phases in mutual equilibrium. Diffraction lines of the α(M/β)-phase were shifted to higher Bragg angles as compared to pure Al, due to remaining Zn in the matrix. The unit-cell parameter of the α(M/β)-phase at RT (298 K) was independent of the alloy composition, x(Zn) (within the experimental error), amounting a[α(M/β)] = 0.40445(10) nm, which was smaller for 0.12 % than that of Al, a(Al). Also, the alloys with a small x(Zn), 0.03, 0.045 and 0.08, quenched from T_t to RT aged at 520 K and very slowly cooled to RT (specimens WQASC) showed practically that same value of the unit-cell parameter. Diffraction lines of the β-phase were close to positions of those of pure Zn. The measured unit-cell parameters of the β-phase were a(β) = 0.2665(2), c(β) = 0.4947(3) nm, c(β)/a(β) = 1.856(3) at RT (298 K), space group being $P6_3mmc$. Diffraction lines of both phases, α(M/β) and β, were rather sharp, indicating that the annealing of most strains in the crystal lattice took place during slow cooling. The orientation relationship between the β precipitates and the host α(M/β)-phase was: {001}β||{111}α, $[110]\beta \| [1\,\bar{1}0]\alpha$.[2,6]

Microstructure of As-quenched Alloys

In the as-quenched Al-Zn alloys (specimens WQ), which were supersaturated solid solutions, decomposition processes and formation of precipitates took place immediately after quenching. In these alloys the Zn atoms (or clusters of Zn atoms) were not randomly distributed in the Al host crystal lattice, due to lattice defects, such as grain boundaries, dislocations (dislocation loops), stacking faults, vacancies, Zn-vacancy pairs.

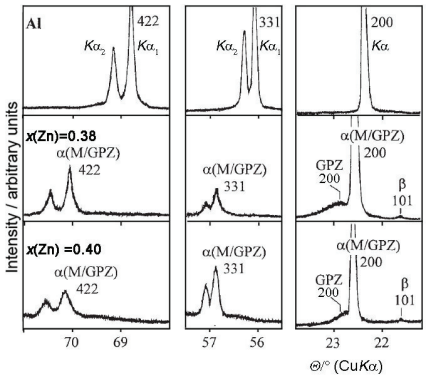

Figure 1. Characteristic X-ray diffraction lines of pure aluminium and of Al-Zn alloys having the zinc fraction, x(Zn), 0.38 and 0.40 (all fine powder). Aluminium was slowly cooled, while the Al-Zn alloys were quenched from T_t to RT. XRD lines of the alloys were scanned within 30 minutes after quenching. Diffraction effect from GPZ is indicated.[8]

These facts are important for homogenous (GPZ and β precipitates) and discontinuous/heterogeneous (β precipitates) modes of decomposition of supersaturated solid solutions, *i.e.* for nucleation of precipitates.[2] The first precipitates were GPZ in alloys with the Zn atomic fraction, $x(\mathrm{Zn}) \leq 0.44$. In the alloys with a higher x(Zn), the decomposition process was very fast and the sequence of precipitates was shortened. The decomposition rate and formation of GPZ also depends on the quenching rate, that is, on the quenched-in vacancies, and on the ageing temperature, which strongly influence the diffusion of Zn atoms inside the host α-phase crystal lattice.[2,6,7]

As an example, characteristic parts of XRD patterns of the WQ alloys, having x(Zn) = 0.38 and 0.40, including diffraction lines at low and high Bragg angles, are shown in Figure 1. For comparison, the same diffraction lines of pure Al are also shown in Figure 1. Diffraction line profiles were scanned within 30 minutes after quenching. These diffraction patterns corresponded to two-phase alloys, namely, the α-phase (the matrix), denoted as α(M/GPZ), and a dense system of GPZ, which were in mutual metastable equilibrium. It is obvious from Figure 1, that diffraction lines of α(M/GPZ), being rather sharp and well resolved in the spectral $K\alpha_1$ and $K\alpha_2$ components, were shifted to higher Bragg angles in relation to those of pure Al. That shift increased with x(Zn). The mean diameter of the initially precipitated GPZ in the alloys with x(Zn) = 0.24 was about 2 nm (as found from XRD line broadening and TEM), and the mean separation of adjacent zones was about 8 to 10 nm (as found from SAXS).[5] Therefore, the initial volume fraction of GPZ was ≈ 1 % of the alloy volume. It follows that most of Zn content in the alloy was solved in the α(M/GPZ)-phase, causing the shift of its diffraction lines, and only small fraction of Zn participated in GPZ, in spite that GPZ were composed of ≈ 70 at% Zn.[2]

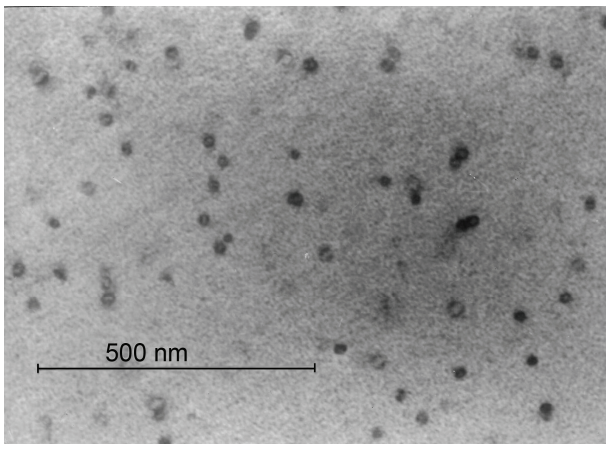

Figure 2. Transmission electron microscopy photograph of the Al-Zn alloy having x(Zn) = 0.08. The alloy was quenched to RT and aged at 350 K for 1 day. Initial GPZ and dislocation loops are visible. A line of zero diffraction contrast across the dislocation loops can be noticed.[5]

The presence of GPZ in as-quenched alloys was manifested as broad humps at the high-angle side of diffraction lines of the α(M/GPZ)-phase. These diffraction effects in GPZ are shown in Figure 1 for the alloys with x(Zn) of 0.38 and 0.40. The unit-cell parameter of fcc GPZ was smaller than that of α(M/GPZ) due to a much higher Zn content, while pronounced broadening of GPZ diffraction lines indicated their small sizes. Similar diffraction effects in GPZ were observed by Simerska and Synecek in studying of single crystals of Al-Zn alloys.[13]

A dense system of GPZ and small dislocation loops in the alloy with x(Zn) = 0.08, aged at 350 K for 1 day after quenching, is shown in a transmission electron microscopy (TEM) photograph, Figure 2.

β-phase was not present in the as-quenched alloys having $x(\mathrm{Zn}) \leq 0.44$. The strongest diffraction line of the β-phase, β101, was hardly visible in Figure 1, due to small number of β precipitates, nucleated during the scan of diffraction pattern.

Characteristic parts of diffraction patterns of as-quenched Al-Zn alloy (specimen WQ) with x(Zn) = 0.48 are shown in Figure 3. No diffraction effect from GPZ could be noticed. Instead, strong diffraction lines of the β-phase, nucleated immediately after quenching, were present. Diffraction lines of the α(M/β)-phase were rather broad, due to strains around β precipitates, the broadening pronouncedly increased with the Bragg angle (*e.g.* diffraction lines α331, α422). For comparison, diffraction lines of the same alloy, slowly cooled from T_t (specimen SC) are also shown in Figure 3. One can notice that diffraction lines at high Bragg angles of the SC specimen were rather sharp and resolved in the spectral $K\alpha_1$ and $K\alpha_2$ components. Unit-cell parameters of both α(M/β)- and β-phases of the alloy with x(Zn) = 0.48 differed a little for the WQ and SC specimens due to different Zn content, as can be seen by inspection of Figure 3.

The unit-cell parameter of the as-quenched alloys, a[α(M/GPZ)], in dependence on the initial Zn fraction, x(Zn) is shown in Figure 4. These values averaged over the Debye-Scherrer and counter diffractometer data, indicate that the unit-cell parameter of the α(M/GPZ)-phase decreased almost linearly with the increase of x(Zn). This dependence was in a fair agreement with the data given in the literature;[2] however, the previous literature data were available only for $x(\mathrm{Zn}) < 0.30$.

The dependence shown in Figure 4 may be explained in terms of the increased fraction of Zn dis-

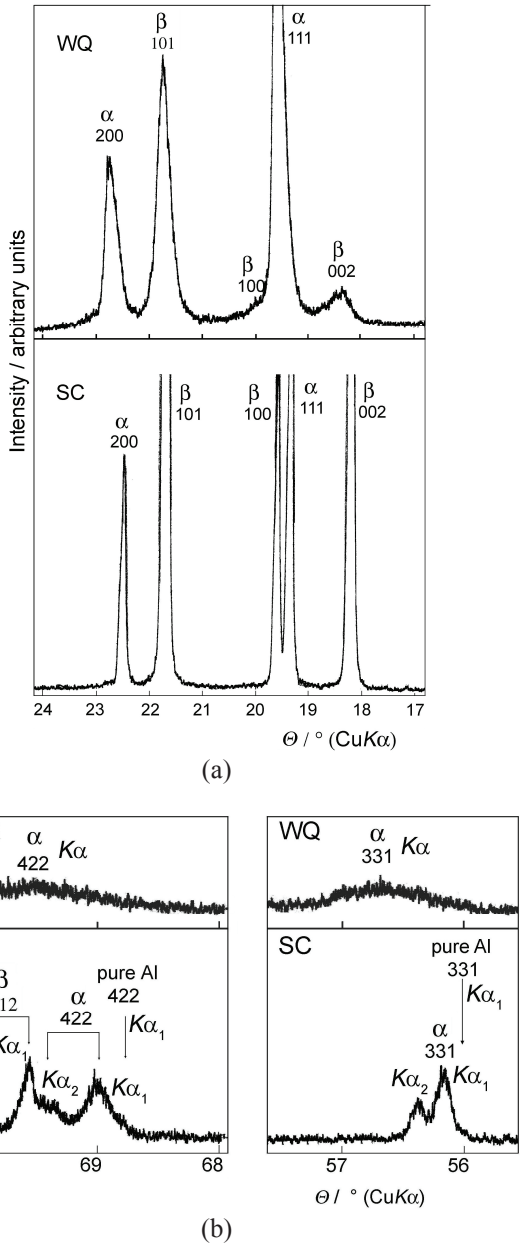

Figure 3. Characteristic parts of XRD pattern of the quenched and slowly cooled Al-Zn alloy having x(Zn) = 0.48 (fine powder); (a) low Bragg angles, (b) high Bragg angles. Diffraction lines of the alloy, that was quenched from T_t to RT, were scanned within 30 minutes after quenching.

solved in the matrix crystal lattice during quenching. For the alloy having x(Zn) = 0.44, the unit-cell parameter of α(M/GPZ) was ≈ 1.0 % smaller than that of pure Al. In the alloys containing a dense system of spherical (or almost spherical) GPZ, coherent with the α(M/GPZ)-phase, there should be a continuation of the crystal lattice planes in GPZ into the crystal lattice of the α-phase, strained around GPZ due to the difference in their unit-cell parameters.

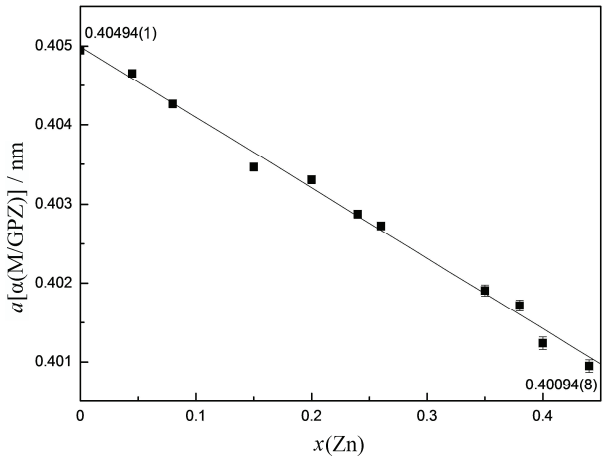

Figure 4. The unit-cell parameter a of the α(M/GPZ)-phase in the Al-Zn alloys, that were quenched from T_t to RT. The values were averaged over the Debye-Scherrer (samples: needles) and counter diffractometer (samples: fine powder) data. Debye-Scherrer patterns were taken within 3 hours, while counter diffractometer patterns within 30 minutes after quenching. The unit-cell parameter of Al is also shown. Vertical bars indicate estimated standard deviations.

Ageing of the Supersaturated Solid Solutions

The alloys with x(Zn) ≤ 0.44, that had been rapidly quenched from T_t to RT, were two-phase systems (as described above), in which the α(M/GPZ)-phase was in a metastable equilibrium with a dense system of spherical GPZ (specimens WQ). During ageing of these alloys, at RT or at elevated temperature (up to 350 K), diffraction lines of the α(M/GPZ)-phase gradually decreased in intensity; becoming little broader, but did not change their angular positions. At the same time, diffraction lines of α(M/β)-phase appeared at Bragg angles close to those of the α(M/β)-phase in the slowly cooled alloys (specimens SC), as well as diffraction lines of the β-phase at Bragg angles very close to those of the β-phase in the slowly cooled alloys. Diffraction lines of the two phases, α(M/GPZ) and α(M/β), having the same indices, were separated in diffraction pattern because of different unit-cell parameters of the two phases, due to different Zn fraction retained in them; that separation increased with the initial Zn fraction, x(Zn). Diffraction lines of both α(M/β)- and β-phases practically did not move during the whole ageing treatment. GPZ grew in size with ageing at first, but, having reached a size of, say, ten nanometers and becoming ellipsoidal,[14] they transformed to the β precipitates. In parallel to that process, β precipitates discontinuously/heterogeuously nucleated at dislocation loops, grain boundaries and other lattice defects. For instance, β precipitates appeared in XRD patterns in the alloy with x(Zn) = 0.24 after 24 hours of ageing at RT.

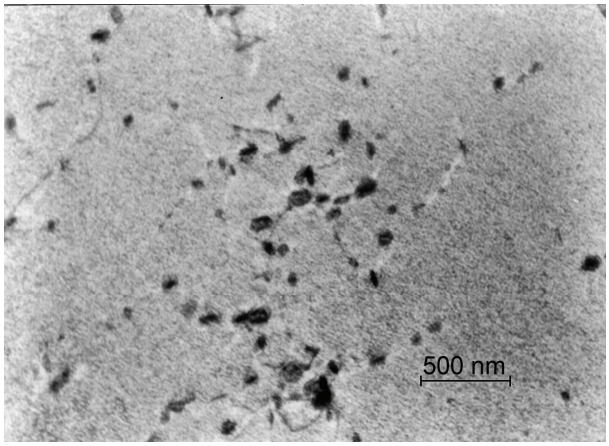

Figure 5. Transmission electron microscopy photograph of the Al-Zn alloy having x(Zn) = 0.08. The alloy was quenched to RT and aged at 350 K for 30 days. GPZ and initial β precipitates are visible.[5]

A dense system of GPZ and initial β precipitates in the alloy with x(Zn) = 0.08, that had been quenched from T_t to RT and aged for 30 days at 350 K, is shown in Figure 5.

At short ageing intervals, diffraction lines of the α(M/β)-phase were very broad, because of strains around the β precipitates. The broadening increased with the Bragg angle. As ageing proceeded, diffraction lines of the α(M/β)-phase became sharper and their intensity increased due to an increase of its volume fraction and a partial annealing of strains around the β precipitates. For a prolonged ageing, diffraction lines of the α(M/β)-phase finally were partially resolved into the spectral components $K\alpha_1$ and $K\alpha_2$. Diffraction lines of the α(M/GPZ)-phase became little broader, due to strains introduced by coarsening of GPZ, and, at later stages of ageing, due to decreasing of its crystallite sizes. The number and size of the β precipitates gradually increased with the ageing time, as indicated by the increase of diffraction line intensities. The diffraction lines of the β-phase were rather sharp even at very short ageing times indicating negligible strains in its crystal lattice.

As mentioned above, a number of the β precipitates were nucleated at GPZ. That transition might start with the formation of the hcp sequence (*i.e.* stacking faults) of the {111} planes of GPZ resulting in thin lamellae of the β-phase structure inside GPZ; with the orientation relationship {001}β||{111}GPZ, in accordance with the one between α(M/β)- and β-phases. From the unit-cell parameters of the α(M/β)- and β-phases, the misfit of these two phases was $\left|3c(\beta) - 2\sqrt{3}a[\alpha(\mathrm{M}/\beta)]\right| \approx 5.5\,\%$. Due to that rather small misfit, some of the {001}β planes of thin β-platelets might be continued into the α(M/β)-phase as the {111}α planes, maintaining a certain degree of coherency and causing strained crystal lattice of the α(M/β)-phase around the β-platelets. As the ageing time proceeded on, β precipitates grew in size and the mutual coherency along the α(M/β) and β interfaces was more and more destroyed. Micrometer sized β precipitates were not coherent with the host α(M/β)-phase.

As an example, the transition of the metastable two-phase system, α(M/GPZ)+GPZ, into a more stable two-phase system, α(M/β)+β, in the alloy with x(Zn) = 0.38 in shown in Figure 6: 30 minutes after quenching diffraction lines of the α(M/GPZ)-phase and broad humps of GPZ were present; for the ageing time of 52.5 hours at RT the alloy contained phases α(M/GPZ), α(M/β), GPZ and β; after a prolonged ageing for 35 days at RT the alloy approached the equilibrium state, consisting of the α(M/β)-phase and β precipitates. One can notice the difference in broadening between the corresponding diffraction lines of the phases α(M/GPZ) and α(M/β), as described above.

The decomposition rate of the metastable two-phase alloy, α(M/GPZ)+GPZ, into a more stable two-phase alloy, α(M/β)+β, increased with the Zn fraction, x(Zn). For the alloy with x(Zn) = 0.24 aged at RT, diffraction line intensities of the β-phase reached a satu-

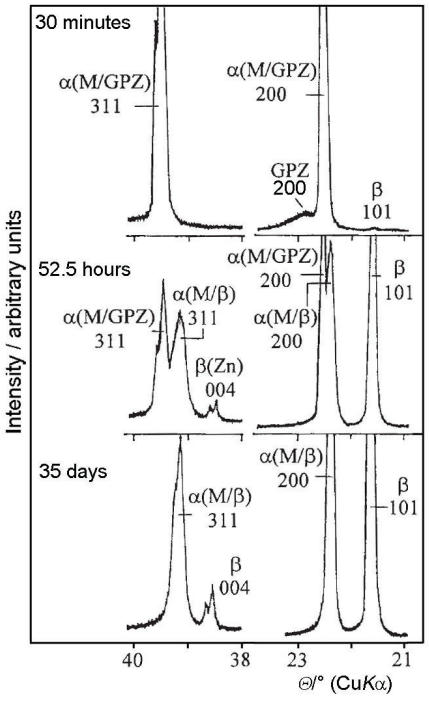

Figure 6. Characteristic diffraction lines of the Al-Zn alloy having x(Zn) = 0.38 (fine powder). The alloy was quenched from T_t to RT and aged at RT for 30 minutes, 52.5 hours and for 35 days. A gradual transition from the metastable two-phase system, α(M/GPZ) + GPZ, into a more stable two-phase system, α(M/ β) + β, can be noticed.[8]

ration after 3 months, but a gradual sharpening of diffraction lines of the α(M/β)-phase was noticed even after 7 months. The corresponding processes for the alloy with x(Zn) = 0.44 lasted several days. On the contrary, for the alloy with x(Zn) = 0.08, GPZ did not transform to β precipitates at RT. For ageing at 350 K, the decomposition process in that alloy was very slow, and the intensities of the β-phase diffraction lines did not reach saturation even after 8 months.

The intensities of diffraction lines of the β-phase, as mentioned above, increased with the ageing time. For instance, for the alloy with x(Zn) = 0.24, the increase of diffraction-line intensities of the β-phase was enhanced after 3 to 4 days, due to a direct transition of GPZ into β precipitates, this process taking place in parallel to discontinuously nucleated β precipitates. Finally, diffraction line intensities of the β-phase approached values corresponding to the ones of the slowly cooled alloys.[6]

After a prolonged ageing, the Bragg angles of rather sharp diffraction lines of the α(M/β)-phase, being in coexistence with the β-phase, were very similar for all studied alloys. It followed that the unit-cell parameter of the α(M/β)-phase was independent on the alloy initial Zn fraction, x(Zn), amounting a[α(M/β)] = 0.40469(6) nm, and being for 0.06 % smaller than the one of pure Al. It was shown that the unit-cell parameter a[α(M/β)] in the slowly cooled alloys differed from that of pure Al for 0.12 %. That difference in the unit-cell parameter of the two α(M/β)-phases may be explained in terms of different thermal treatments, causing a different fraction of Zn retained in the host crystal lattice.

A more detailed description of the processes taking place during ageing of the quenched alloys is given in previous papers.[5,6]

Temperature Dependence of Microstructure of the Quenched-aged and Slowly Cooled Alloys

As mentioned above, two different thermal treatments of the alloys were applied in order to approach the equilibrium two-phase state, namely α(M/β)+β: (i) rapid quenching from $T_t > T_{ss}$ to RT and prolonged ageing (specimens WQPA); (ii) slow cooling from $T_t > T_{ss}$ to RT (specimens SC). The microstructure of these alloys was studied *in situ* by XRD during slow heating from RT to T_t and slow cooling back to RT. The alloys with the following initial Zn fraction, x(Zn), were examined: 0.08, 0.24, 0.40, 0.44, 0.48, 0.54 and 0.62. The temperature dependence of the microstructure of the alloys with x(Zn) ≤ 0.40 was in a fair accordance with the phase diagram of the Al-Zn system, accepted in the literature (the solid and dash-dot lines in Figure 7[2,4]), while the one of alloys with x(Zn) ≥ 0.44 was not. For that reason, the two groups of alloys are described separately in the following part of the paper. The results, given in the present paper on the temperature behavior of the microstructure of the alloys with x(Zn) ≥ 0.44, represent a slight modification of statements given in the previous papers.[7,8]

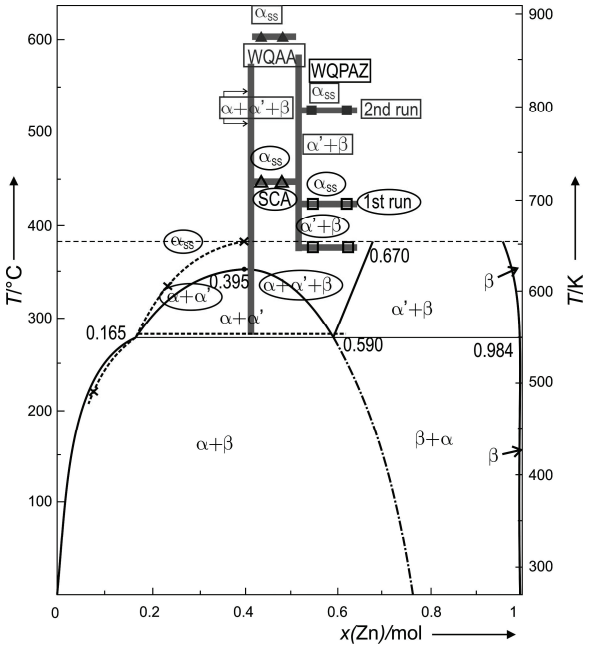

Figure 7. The sketch of the phase diagram of the system Al-Zn. The solid and dash-dot lines are related to the diagram as accepted in the literature[2,4] (shown here in a simplified form), with the existing phases and the characteristic x(Zn) values indicated; this diagram is shown only up to 650 K (dashed line, parallel to the abscisa axis). The data from the present work are shown with crosses [x(Zn) = 0.08, 0.24, 0.40; samples SCA], triangles [x(Zn) = 0.44, 0.48; empty triangles - samples SCA; full triangles – samples WQAA] and squares [x(Zn) = 0.54, 0.62: samples WQPAZ; empty squares – the first heating run, full squares – the second heating run]. The curved dashed line [in the region x(Zn) ≤ 0.40] and wide gray lines [in the region x(Zn) ≥ 0.40] indicate approximately the proposed phase boundaries, which replace solid lines of the literature phase diagram. The existing phases are given in ellipses and rectangles.

The Al-Zn Alloys with x*(Zn) ≤ 0.40*

Characteristic parts of XRD patterns of the alloys having x(Zn) = 0.24 and 0.40, taken at a series of temperatures (including both heating and cooling runs), as well as the temperature dependence of the Bragg angle and the relative intensity of prominent diffraction lines of the phases present in the same alloys, were shown in a previous paper (Figures 1–4).[7] The temperature dependence of microstructure was rather similar for both slowly cooled (SCA) and quenched and prolongedly aged (WQPAA) alloys; therefore, the following description on the main observations is related to both thermal treatments.

A gradual increase of the temperature caused a decrease in intensities of diffraction lines of both α(M/β)- and β-phases, due to enhanced vibration amplitudes of the atoms. A shift of diffraction lines toward smaller Bragg angles was observed, due to thermal expansion; that change was linear up to ≈ 490 K. At higher temperatures, a partial dissolution of the β precipitates in the α(M/β)-phase took place; that effect compensated or even reversed the shift of the α(M/β)-phase diffraction lines due to thermal expansion, as the Zn atoms are smaller than the Al atoms. The dissolution of the β-phase was manifested in an enhanced decrease of its diffraction line intensities.

As the temperature increased slightly above 550 K, a phase transition of the β-phase into an fcc phase, denoted as α', took place. Namely, diffraction lines of the β-phase abruptly disappeared for the alloys with x(Zn) = 0.24, and 0.40, while at the same time diffraction lines of the α'-phase appeared at the high-angle side of all α-phase diffraction lines; the α-phase being now in a metastable equilibrium with α'-phase and therefore denoted as α(M/α'). According to the phase diagram (Figure 7[2,4]) the β→α' phase transition takes place at 550 K (Figure 7, solid line parallel to the abscisa axis). Our DSC study of the alloy with x(Zn) = 0.24 gave the value of 555 K for the β→α' phase transition (Figure 8a), in line with XRD results (Figure 7, dashed line parallel to the abscisa axis). From the difference between the Bragg angles of the corresponding diffraction lines of the α(M/α')- and α'-phases at 560 K, one could conclude that the unit-cell parameter of the α'-phase was about 0.9 % smaller than the one of the α(M/α')-phase, due to a much higher Zn fraction contained in the α'-phase; the details were given in the previous paper.[7] The curve showing the temperature dependence of the relative difference of the unit-cell parameters of the α(M/α')- and α'-phases ran parallel to the curve showing the temperature dependence of the difference in the Zn fractions contained in the two phases.[7] One may conclude that the relative difference in the unit-cell parameters between the α(M/α')- and α'-phases and its dependence on temperature was dominantly determined by the difference between their Zn-fractions, and to a much smaller degree by the coherency strains. At a given temperature, diffraction line intensities of the α'-phase were bigger, the higher x(Zn) was. The average intensity ratio of the corresponding diffraction lines of the α(M/α')- and α'-phases was > 1 for x(Zn) = 0.24 and < 1 for x(Zn) = 0.40 at ≈ 560 K.

With a further increase of temperature, above 555 K, diffraction lines of the α(M/α')-phase and the corresponding diffraction lines of the α'-phase moved toward each other. These shifts were due to a decrease of the Zn fraction in the α'-phase and an increase of the Zn fraction in the α(M/α')-phase. However, in the temperature interval of the existence of the α'-phase, the Bragg angles of its diffraction lines did not depend on x(Zn), and the same conclusion was valid for the α(M/α')-phase diffraction lines. The diffraction line intensities of the α'-phase decreased with the increase of the temperature.

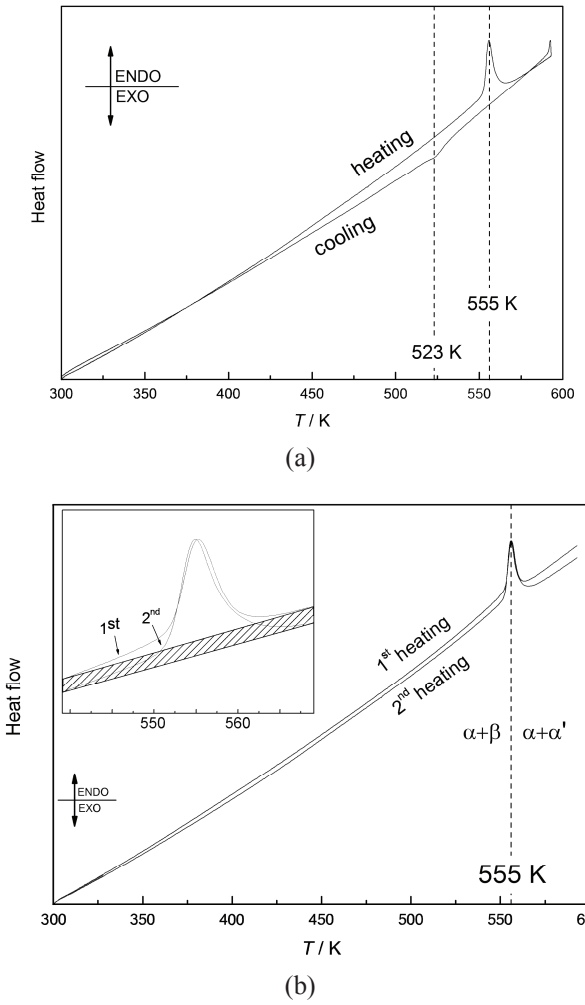

Figure 8. DSC curves of the Al-Zn alloy (fine powder), having x(Zn) = 0.24; (a) for the first heating run and the first cooling run, with the temperatures of the phase transitions β → α' and α' → β indicated; (b) for the first heating run and for the second heating run, with the temperature of the phase transition β → α' indicated, the inset showing an enlarged region of the phase transition.

In a fair accordance with the phase diagram, the solid solution of Zn in Al was formed at T_{ss} ≈ 615 K for the alloy with x(Zn) = 0.24, and at T_{ss} ≈ 655 K for the alloy with x(Zn) = 0.40 (crosses connected with the curved dashed line in Figure 7); diffraction lines of the α'-phase were present no more. Therefore, the sequence of phase transitions during heating the alloys from RT to T_t was: α(M/β) + β → α(M/α') + α' → α_{ss}.

The phase transition β→α' was not observed for the alloy with x(Zn) = 0.08; for that alloy the solid solution was formed at $T_{ss} \approx 495$ K (shown by a cross in Figure 7), in line with the phase diagram. As the temperature increased, the β-phase gradually dissolved in the α(M/β)-phase, and its diffraction lines disappeared with approaching the solid solution temperature.

The unit-cell parameter, $a(\alpha_{ss})$, of the solid solution depended on x(Zn); it decreased as x(Zn) increased. The following values of $a(\alpha_{ss})$ were found at 673 K: 0.40925(8), 0.40824(7) and 0.40692(9) nm for x(Zn) = 0.08, 0.24 and 0.40, respectively. The unit-cell parameter of pure Al was found to be 0.40952(6) nm at 673 K.

In the temperature interval of its existence, the β-phase exhibited a pronounced anisotropy in thermal expansion. As its diffraction pattern did not show intense 00*l* diffraction lines at higher Bragg angles, diffraction lines of the type *hkl*, with *l* dominant in relation to *h* and *k*, were utilized in measurement of the unit-cell parameter *c*. The anisotropy in thermal expansion was manifested, for instance, in increased angular separation of diffraction lines 110 and 103, as the temperature increased. Supposing a linear change of the Bragg angles of diffraction lines with temperature, the average thermal expansion coefficients, γ, of the β-phase in the interval from RT to 555 K for the studied alloys were: $\gamma[110] = 1.1(1) \times 10^{-5}$ / K, $\gamma[103] = 5.8(5) \times 10^{-5}$ / K. It followed: $\gamma[001] = 8.5(9) \times 10^{-5}$ /K.

During the cooling run, from T_t to RT, the studied alloys underwent the inverse phase transitions, $\alpha_{ss} \rightarrow \alpha' + \alpha(M/\alpha') \rightarrow \beta + \alpha(M/\beta)$, but exhibiting a temperature hysteresis. For instance, the phase transition α'→β for the alloy with x(Zn) = 0.24 took place at 523 K, what was 32 K below the temperature of the transition β→α' in the heating run, as can be seen in Figure 8a. It can be also noticed from DSC curves in Figure 8a, that the transition α'→β was spread over a much bigger temperature interval than the transition β→α'. A repeated, second, heating of the same specimen of the alloy with x(Zn) = 0.24 showed that the temperature of the phase transition β→α' was practically the same to that in the first heating as shown in Figure 8b. One can notice in Figure 8b, that the background line of the DSC curve in the second heating was lower than the one in the first heating, probably due to partially annealed strains during the first heating and cooling cycle.

At a given temperature, the Bragg angles of the α'-phase diffraction lines in the cooling run were very similar to those in the heating run, not depending on x(Zn). The fractions of Zn in the β- and α(M/β)-phases, and in the α'- and α(M/α')-phases, while in mutual equilibrium, in dependence on the temperature, are given in Ref. 2, 4, 7.

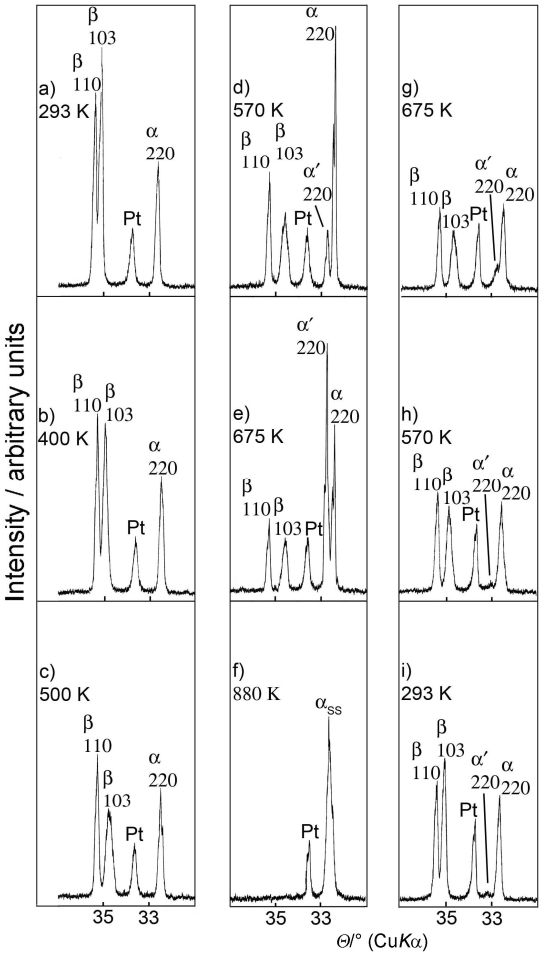

Figure 9. Characteristic XRD lines of the Al-Zn alloy (fine powder) having x(Zn) = 0.44, at selected temperatures during the heating and the cooling cycle. Prior to XRD study at high temperature, the alloy was quenched from T_t to RT and aged at RT for 11 months.

The Al-Zn/Zn-Al Alloys with x*(Zn)* ≥ *0.44*

According to the phase diagram, accepted in the literature (Figure 7, solid and dash-dot lines), the following phase transitions could be expected:

(i) for the alloys having x(Zn) = 0.44, 0.48 and 0.54,

$$\alpha(M/\beta) + \beta - \alpha(M/\alpha') + \alpha' - \alpha_{ss}$$

(ii) for the alloy having x(Zn) = 0.62,

$$\alpha(M/\beta) + \beta - \alpha' + \beta - \alpha_{ss}$$

However, the following sequence of phase transitions was observed for the alloys having x(Zn) = 0.44 and 0.48 (in which Al was the major element; Figure 7, the present experimental data shown by triangles, the observed phases given in ellipses/rectangles, the proposed phase boundaries shown by wide gray lines):

$$\alpha(M/\beta) + \beta - \alpha(M/\alpha',\beta) + \alpha' + \beta - \alpha_{ss}$$

On the other hand, for the alloys having x(Zn) 0.54 and 0.62 (in which Zn was the major element), the following phase transitions were observed (Figure 7, the present experimental data shown by squares, the observed phases given in ellipses/rectangles, the proposed phase boundaries shown by wide gray lines):

$$\alpha(M/\beta) + \beta - \alpha(M/\alpha',\beta) + \alpha' + \beta - \alpha' + \beta - \alpha_{ss}$$

Characteristic parts of XRD patterns of the alloy with x(Zn) = 0.44 at selected temperatures are shown in Figure 9. That alloy was quenched from T_t to RT and prolongedly aged, for 11 months, at RT (WQPAA) prior to XRD study *in situ* at high temperature. Similarly, characteristic parts of XRD patterns of the alloy with x(Zn) = 0.48 at selected temperatures are shown in Figure 10, including both the first and second heating and cooling cycles. That alloy was quenched from T_t to RT and aged at RT for one week (WQAA) prior to XRD study *in situ* at high temperature.

The unit-cell parameter of the α(M/β)-phase, in equilibrium with the β-phase, approached (asymptotically) after a prolonged ageing of the quenched alloys (WQPAA, WQPAZ), did not depend on x(Zn), amounting 0.40469(8) nm at RT. For the slowly cooled alloys (SCA), the unit-cell parameter of the α(M/β)-phase at RT was 0.40445(10) nm, regardless of x(Zn). The above values were the same as the ones for the alloys with x(Zn) ≤ 0.40. Also, the unit-cell parameters of the β-phase, in equilibrium with the α(M/β)-phase, were very close to those of pure Zn at RT, as mentioned in discussion on the alloys with x(Zn) ≤ 0.40.

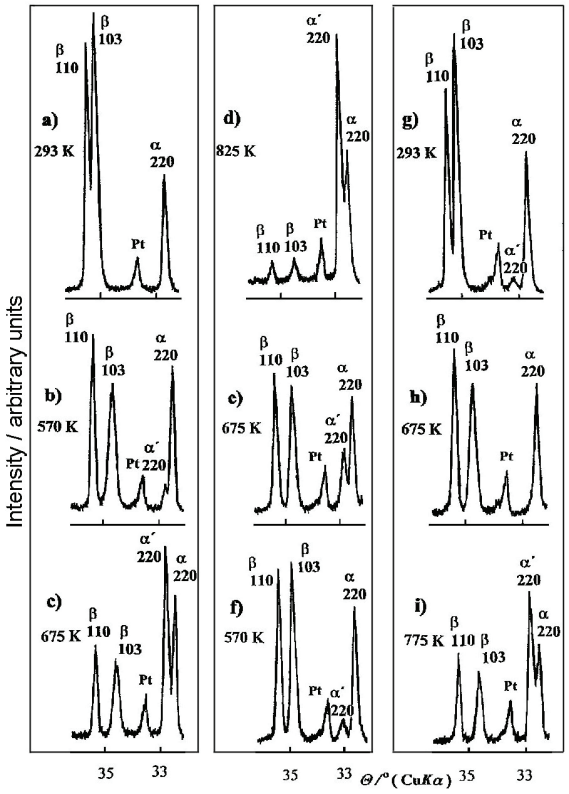

Figure 10. Characteristic XRD lines of the Al-Zn alloy (fine powder) having x(Zn) = 0.48, at selected temperatures, including both the first and second heating and cooling cycles. Prior to XRD study at high temperature, the alloy was quenched from T_t to RT and aged at RT for one week.

Figures 11, 12 and 13 correspond to the alloy with x(Zn) = 0.48, that was (i) quenched from T_t to RT and aged for one week at RT (WQAA), (ii) slowly cooled from T_t to RT (SCA). Figure 11 shows the temperature dependence of the unit-cell parameter a of the phases α, α' and α_{ss} during the first heating and cooling cycle. The direction of temperature change is indicated by arrows, and vertical bars show the estimated standard deviation in the derived parameter values. The same features are also applied in the following figures, 12–14. The temperature dependence of the unit-cell parameters a(β) and c(β) of the β-phase is shown in Figures 12 and 13, re-

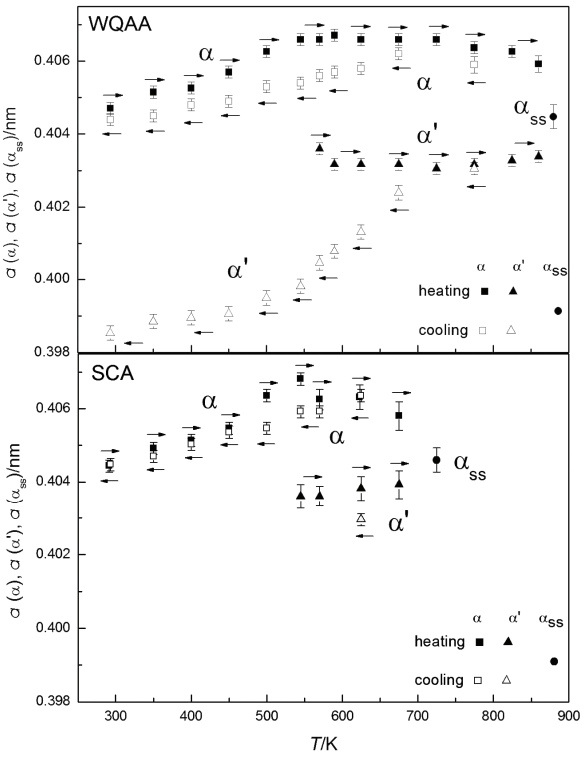

Figure 11. Temperature dependence of the unit-cell parameter a of the phases α, α' and α_{ss} in the Al-Zn alloy having x(Zn) = 0.48 during the first heating and cooling cycle. The upper part is related to the alloy that was quenched from T_t to RT and aged for one week at RT prior to XRD study at high temperature. The lower part is related to the alloy that was slowly cooled from T_t to RT prior to XRD study at high temperature. Arrows indicate the sense of temperature change, and vertical bars estimated standard deviation in a.

spectively, during the first heating and cooling cycle. Figure 14 shows the temperature dependence of an interplanar spacing of the β-phase, namely d_{103} (which is of a particular interest, including the temperature behavior of both the *a* and *c* crystal axes) in the alloy with x(Zn) = 0.44. That alloy was quenched from T_t to RT and aged at RT for 11 months (WQPAA). Analogous temperature dependence of microstructure was observed for the alloys in which Zn was the major element (quenched from T_t to RT, aged at RT, prior to XRD study *in situ* at high temperature, WQPAZ).

The temperature dependence of XRD patterns, and therefore the microstructure of the quenched alloys (WQAA, WQPAA, WQPAZ) was rather different from that of the slowly cooled alloys (SCA), as follows from Figures 11–13. The two curves, which show that dependence during the first heating from RT to T_t and cooling back to RT, were closer to each other for the slowly-cooled alloys than for the quenched alloys. That is, the area between the two curves was smaller for the slowly-cooled alloys than for the quenched alloys. That area slightly increased with the increase of x(Zn). For the quenched alloys, the curves corresponding to the second heating from RT to T_t and second cooling from T_t to RT were close to the ones of the first cooling from T_t to RT; these curves can be approximated by a linear function, (*e.g.* Figure 14). On the other hand, the curves corresponding to the first heating from RT to T_t were quite different, much deviating from the linear function (*e.g.* Figure 14). At a given temperature, the difference between the values of a microstructural parameter, found in the heating run and in the cooling run, was smaller for the slowly-cooled alloys than for the quenched alloys (*e.g.* Figures 11–13); that difference slightly decreased with the prolonged ageing of one and the same alloy (for instance, specimens WQPAA *vs.* specimens WQAA).

General features observed in XRD patterns were as follows. As the temperature of a given alloy increased a decrease of the diffraction line intensities of both α(M/β)- and β-phases took place, due to enhanced vibration amplitudes of the atoms. Thermal expansion manifested in a gradual shift of diffraction lines toward smaller Bragg angles. Thermal expansion of the β-phase was anisotropic as in case of the alloys with x(Zn) ≤ 0.40.

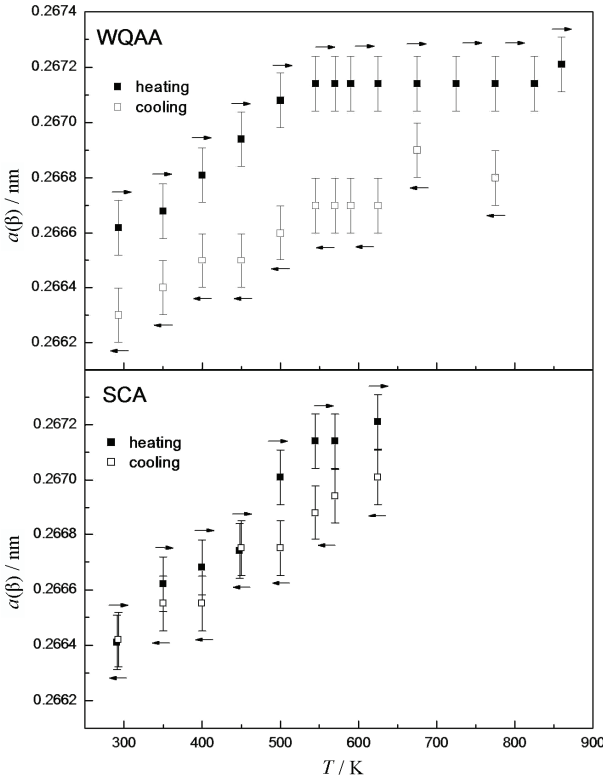

Figure 12. Temperature dependence of the unit-cell parameter *a* of the β-phase in the Al-Zn alloy having x(Zn) = 0.48, during the first heating and cooling cycle. The upper part is related to the alloy that was quenched from T_t to RT and aged at RT for one week prior to XRD study at high temperature. The lower part is related to the alloy that was slowly cooled from T_t to RT prior to XRD study at high temperature. Arrows indicate the sense of temperature change, and vertical bars the estimated standard deviation in *a*(β).

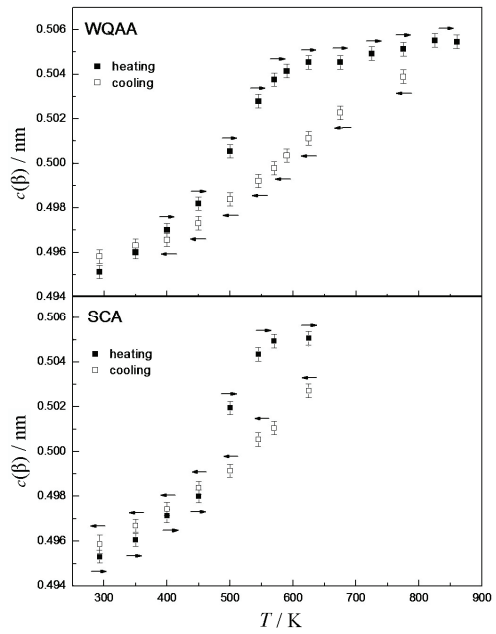

Figure 13. Temperature dependence of the unit-cell parameter *c* of the β-phase in the Al-Zn alloy having x(Zn) = 0.48, during the first heating and cooling cycle. The upper part is related to the alloy that was quenched from T_t to RT and aged at RT for one week prior to XRD study at high temperature. The lower part is related to the alloy that was slowly cooled from T_t to RT prior to XRD study at high temperature. Arrows indicate the sense of temperature change, and vertical bars the estimated standard deviation in *c*(β).

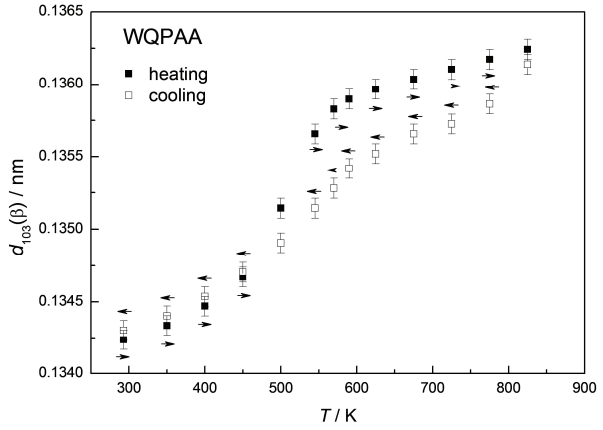

Figure 14. Temperature dependence of the interplanar spacing d_{103} of the β-phase in the Al-Zn alloy having x(Zn) = 0.44, during the first heating and cooling cycle. The alloy was quenched from T_t to RT and aged for 11 months at RT prior to XRD study at high temperature. Arrows indicate the sense of temperature change, and vertical bars estimated standard deviation in d_{103}.

It could be followed, *e.g.*, from the temperature dependence of the angular separation of neighboring diffraction lines, β110 and β103 (Figures 9, 10). An indication of thermal expansion anisotropy may also be a decrease of the saddle intensity between diffraction lines β110 and β103 (Figures 9, 10).

The unit-cell parameter, a, of the α(M/β)-phase, for both quenched and slowly cooled alloys, increased almost linearly during the first heating run up to 490–500 K (Figure 11). At a higher temperature, a partial dissolution of Zn from β precipitates into the α(M/β)-phase took place. That process compensated and even reversed the change of the unit-cell parameter of the α(M/β)-phase due to thermal expansion (Figure 11), as the Zn atoms are smaller than the Al atoms. In connection with the dissolution of Zn in the α(M/β)-phase one could observe a change of the shape of the β precipitates with the increase of temperature: the broadening of diffraction lines with $l \neq 0$ (*e.g.* β002, β103) increased in relation to broadening of diffraction lines with $l = 0$ (*e.g.* β100, β110). β precipitates became more and more flat, *i.e.* their dimension along c-axis decreased as the temperature increased. Zn atoms, which left the β precipitates and dissolved in the α(M/β)-phase, were dominantly those which form the lattice planes β{001}. That effect was not observed for the alloys having x(Zn) ≤ 0.40. The concentration of vacancies in the β-phase increased with temperature, that affecting the temperature dependence of its unit-cell parameters in the quenched alloys (Figures 12, 13).

As the temperature increased above ≈ 555 K, a new phase, α' (fcc), appeared in line with the phase diagram. The unit-cell parameter, a, of the α'-phase, being rich in Zn, was smaller (0.8 to 0.9 % at 560 K) than the one of the α-phase. Therefore, diffraction lines of the α'-phase were located at the high-angle side of the corresponding diffraction lines (having the same Miller indices) of the α-phase. According to the phase diagram (Figure 7, solid lines), the alloys with x(Zn) = 0.44, 0.48 and 0.54 should contain the α-phase in coexistence with the α'-phase above 555 K, *i.e.* the β-phase should be completely transformed into the α'-phase. The alloy with x(Zn) = 0.62 should contain α'- and β-phases (Figure 7, solid lines). However, our previous[9–11] and present results indicated that only a partial transition of the β-phase, and probably a partial transition of the α(M/β)-phase, into the α'-phase took place above 555 K. Therefore, the α-phase was in coexistence (a metastable equilibrium) with both α'- and β-phases (Figure 7, the observed phases given in ellipses and rectangles; Figures 9, 10), and was denoted as α(M/α',β).

With a further increase of temperature of the quenched alloys, the fraction of Zn in α(M/α',β)-phase, and probably in the α'-phase, increased (Figure 11, WQAA). The Zn atoms came from the β-phase, in which the concentration of vacancies increased, that compensating thermal expansion of the β-phase (Figure 12, WQAA; Figure 13, WQAA). In the slowly cooled alloys, the concentration of vacancies above 555 K was smaller than in the quenched alloys, and the influence on the thermal expansion was small (Figure 12, SCA; Figure 13, SCA). Diffraction line intensities of the α'-phase increased, while those of the β- and α(M/α',β)-phases decreased.

For the alloys having x(Zn) = 0.44 and 0.48, the solid solution, α_{ss} (fcc), was formed at ≈ 880 K for the quenched alloys (Figure 7, full triangles; WQAA, WQPAA), and at ≈ 725 K for the slowly cooled alloys (Figure 7, empty triangles; SCA). The measurement of $a(\alpha_{ss})$ was not so accurate, due to the recrystallization (grain coarsening) effect in the alloys, as the temperature approached T_{ss}; that was manifested in appearance of local maxima in diffraction line profiles (Figure 9f). At 880 K, $a(\alpha_{ss})$ was estimated to 0.4046(1) and 0.4045(1) nm for the quenched alloys (WQAA, WQPAA) with x(Zn) = 0.44 and 0.48, resp. At 725 K, $a(\alpha_{ss})$ was found to be 0.4044(1) and 0.4043(1) nm for the slowly cooled alloys (SCA) having x(Zn) = 0.44 and 0.48, respectively.

On the other hand, for the alloys with x(Zn) = 0.54 and 0.62 (WQPAZ), the α(M/α',β)-phase disappeared at ≈ 650 K in the first heating run and the α'-phase remained in coexistence with the β-phase (Figure 7, empty squares). Solid solution, α_{ss} (fcc), was formed at ≈ 700 K (Figure 7, empty squares). The value of $a(\alpha_{ss})$ at 700 K was estimated to 0.4043(1) and 0.4038(1) nm

for the alloys having x(Zn) = 0.54 and 0.62, resp. During the cooling run, from T_t to RT, a temperature hysteresis in reversal phase transitions was observed. In the repeated, second, heating run of the same specimen a temperature delay in phase transitions of several tens of K was found in relation to the first heating run (Figure 10c,h,i). The α(M/α',β)-phase disappeared at ≈ 720 K, and the solid solution, α_{ss}, was formed at ≈ 800 K (Figure 7, full squares). During the second cooling run to RT, the microstructure showed a similar dependence on temperature as in the first cooling run and in the second heating run.

The alloys with x(Zn) = 0.44 and 0.48 behaved in a similar way during the first cooling run. The intensity of the diffraction lines of the α'-phase decreased in the cooling run more rapidly than it increased in the heating run; at a given temperature the intensity was smaller in the cooling run than in the heating run. The opposite effect was noticed for the β-phase.

Diffraction line intensities of the β-phase, in *e.g.* the quenched alloys (WQPAA), showed three intervals in the first heating run: first, a small decrease due to enhanced vibration amplitudes of Zn atoms, second (above ≈ 500 K), a steeper decrease due to dissolution of Zn atoms from the β-phase into the α(M/β)-phase, third (above ≈ 600 K), a slower decrease toward the formation of solid solution. The behavior during the cooling run was different: after the appearance of the β-phase, the intensities of its diffraction lines increased steeply at first, and that increase slowed down as the temperature decreased toward RT. For the quenched alloys, traces of the α'-phase were observed at RT after a complete heating and cooling cycle (Figures 9, 10, 11).

According to the above results it may be concluded that the value of the unit-cell parameter of the solid solution, $a(\alpha_{ss})$, for the alloys with $0.44 \leq x(\mathrm{Zn}) \leq 0.62$ did not change linearly with x(Zn). These values did not represent a smooth continuation of the values for the alloys with $x(\mathrm{Zn}) \leq 0.40$. The only explanation might be that $a(\alpha_{ss})$ strongly depended on the previous thermal treatment of the alloy, and that some type of ordering was always present even at highest temperatures.

The results described in the present paper indicated that the phase diagram of the system Al-Zn should be modified in its middle part, where the fractions of Al and Zn are comparable, as shown by wide gray lines in Figure 7, proposing boundaries among the observed phases, given in ellipses and rectangles. However, additional studies are needed on the temperature dependence of microstructure in alloys having higher zinc fraction than had alloys studied in the present work.

CONCLUSION

A detailed study of Al-Zn and Zn-Al alloys, having the zinc content, x(Zn), up to 0.62 by XRD, gave many new information on the microstructure of the alloys, in dependence on the initial composition, applied thermal treatment and temperature.

The alloys rapidly quenched from a temperature, T_t, higher than the solid-solution temperature, T_{ss}, to RT were supersaturated solid solutions at RT. When aged, at RT or at a higher temperature, these alloys decomposed, and the precipitation of Guinier-Preston zones (GPZ) and β-phase, as well as the transition of GPZ into the β-phase took place. During ageing, a gradual transition of the α(M/GPZ)-phase, in a metastable equilibrium with GPZ, to the α(M/β)-phase, in an equilibrium with the β precipitates, was followed in detail. The microstructure of the quenched and aged alloys was compared with that of the alloys slowly cooled from T_t to RT. The quenched alloys, being aged for a prolonged time, as well as the slowly cooled alloys, approached an equilibrium state, in which the α(M/β)-phase coexisted with the β-phase. However, the microstructures of the two groups of alloys were different. The slowly cooled alloys were much closer to the stable equilibrium state, than the quenched and aged alloys. In the latter, the precipitates were not uniformly distributed in the crystal lattice of the α(M/β)-phase, and residual strains in the α(M/β)-phase around the β precipitates were present. A very important point was that the quenched-in vacancies at RT were much more numerous in the quenched alloys than in the slowly cooled alloys.

Both quenched and aged alloys and slowly cooled alloys were gradually heated from RT to T_t, and their microstructure was followed *in situ* by XRD; for instance, enhanced thermal vibrations of atoms, thermal expansion, which was found anisotropic for the β-phase, partial dissolution of the β-phase into the α(M/β)-phase, a change of the shape of the β precipitates, phase transition of the β-phase into the α'-phase, or the transition of both β- and α-phase into the α'-phase, coexistence of the α'- and α-phases, or of the α'-, β- and α-phases, a change of composition of particular phases, formation of solid solution. T_{ss} depended on the alloy composition as well as on the thermal treatment. The behavior of the quenched and aged alloys during the temperature change was different from that of the slowly cooled alloys, due to their different starting microstructures at RT, prior to examination by XRD at high temperature. Also, the alloys with $x(\mathrm{Zn}) \leq 0.40$ behaved at high temperature differently than the alloys with $x(\mathrm{Zn}) \geq 0.44$, the behavior of the latter not being in line with the phase diagram, as accepted in the literature.

On cooling the alloys from T_t to RT, a temperature hysteresis was observed in reversal phase transitions; that was also proved by DSC. As the heating and cooling runs were performed slowly, most strains in the quenched and aged alloys were annealed, and the resulting microstructure at RT was different from the starting microstructure at RT, concerning the size and shape of the β precipitates, their distribution in the crystal lattice of the α(M/β)-phase, and the lattice strains around the precipitates. During the repeated, second, heating and cooling runs, the alloys behaved similarly as they did during the first cooling run but a delay of phase transitions was observed in some cases.

A prolonged ageing of the quenched alloys had little influence on the temperature behavior of the alloys. The ideal equilibrium state cannot be reached either by slow cooling from T_t to RT, or by prolonged ageing of RT of the rapidly quenched alloys.

The present study has confirmed the fact, that the quenched-in vacancies, vacancy-Zn pairs and other vacancy complexes play a dominant role in the diffusion rate of Zn atoms. In case the alloy is rapidly quenched (in the present work 10^5 K/s) from a temperature, higher than the solid-solution temperature, to RT, an excess of vacancies is available for the diffusion of Zn atoms. On the other hand, defects in the crystal lattice of the α-phase, such as dislocations, grain boundaries, or incoherent parts of the precipitate–α-phase interface, act as sinks (traps) for vacancies. The precipitation processes, *i.e.* the decomposition of the supersaturated solid solution, depend on the balance of the quenched-in vacancies and traps for vacancies in a particular alloy, subjected to a given thermal treatment.

The present results indicate that a correction of the middle part of the phase diagram of the Al-Zn system is necessary. The reason that final conclusions on that middle part of the pahse diagram cannot be given yet is that T_{ss} depend not only on the alloy composition, but also on the previous thermal treatment. For conclusions, concerning the whole phase diagram, additional studies should be performed on the temperature dependence of microstructure in the alloys with the Zn fraction higher than had the studied alloys.

REFERENCES

1. A. R. West, *Solid State Chemistry and its Applications*, John Wiley&Sons, New York, 1984.
2. H. Löffler, *Structure and Structure Development in Al-Zn Alloys*, Akademie Verlag, Berlin, 1995.
3. L. F. Mondolfo, *Aluminium Alloys: Structure and Properties*, Butterworths & Co. Ltd., London, 1976.
4. H. Löffler, G. Wendrock, and O. Simmich, *Phys. Status Solidi A* **132** (1992) 339–352.
5. S. Popović, H. Löffler, B. Gržeta, G. Wendrock, and P. Czurratis, *Phys. Status Solidi A* **111** (1989) 417–429.
6. S. Popović, B. Gržeta, V. Ilakovac, R. Kroggel, G. Wendrock, and H. Löffler, *Phys. Status Solidi A* **130** (1992) 273–292.
7. S. Popović, B. Gržeta, H. Löffler, and G. Wendrock, *Phys. Status Solidi A* **140** (1993) 341–352.
8. S. Popović and B. Gržeta, *Croat. Chem. Acta* **72** (1999) 621–643.
9. S. Popović, B. Gržeta, B. Hanžek, and S. Hajster, *Fizika A* (Zagreb) **8** (1999) 173–182.
10. Ž. Skoko and S. Popović, *Fizika A* (Zagreb) **10** (2001) 191–202.
11. Ž. Skoko and S. Popović, *Fizika A* (Zagreb) **15** (2006) 61–72.
12. S. Popović, *Cryst. Res. Technol.* **20** (1985) 552–555.
13. M. Simerska and V. Synecek, *Acta Metall.* **15** (1967) 223–230.
14. R. Ramlau and H. Löffler, *Cryst. Res. Technol.* **19** (1984) 1279–1286.

SAŽETAK

Mikrostruktura slitina Al-Zn i Zn-Al

Željko Skoko,[a] Stanko Popović[a] i Goran Štefanić[b]

[a]*Fizički odsjek, Prirodoslovno-matematički fakultet, Sveučilište u Zagrebu, p. p. 331, 10002 Zagreb, Hrvatska*

[b]*Institut "Ruđer Bošković", p. p. 180, 10002 Zagreb, Hrvatska*

Primjenom rentgenske difrakcije istraživana je mikrostruktura naslovnih slitina, s atomnim udjelom Zn, x(Zn), od 0.03 do 0.62, u ovisnosti o sastavu, temperaturi i prethodnoj termičkoj obradi. Slitine su bile: (i) brzo kaljene s temperature T_t, više od temperature čvrste otopine, T_{ss}, u vodu pri sobnoj temperaturi (slitine WQ); (ii) sporo hlađene od T_t do sobne temperature (slitine SC). Neposredno nakon kaljenja slitine WQ su bile čvrste otopine, do x(Zn) ≤ 0.44. Nakon kraćeg starenja, slitine WQ su sadržavale GP zone, bogate cinkom; dugim starenjem te slitine su prevedene u kvazi-ravnotežno stanje i sadržavale su precipitate β, vrlo bogate cinkom. Slitine SC, koje su također sadržavale precipitate β, bile su bliže ravnotežnom stanju nego slitine WQ; mikrostruktura slitina WQ ovisila je o zaostalim deformacijama, zakaljenim prazninama i nejednolikoj raspodjeli precipitata β. Oba niza slitina, SC i dugo starene WQ, grijane su od sobne temperature do T_t, te hlađene na sobnu temperaturu. Tijekom grijanja

je opaženo: smanjenje intenziteta difrakcijskih linija, anizotropija temperaturnog širenja, promjena oblika precipitata, djelomično ili potpuno otapanje precipitata, fazne pretvorbe, stvaranje čvrste otopine. Tijekom hlađenja je uočena temperaturna histereza za obrnute fazne pretvorbe. Temperaturna ovisnost mikrostrukture slitina SC različita je od one dugo starenih slitina WQ. Opažene fazne pretvorbe, za slitine s $x(\mathrm{Zn}) \geq 0.44$, razlikuju se od onih koje predviđa fazni dijagram sustava Al-Zn, prihvaćen u literaturi.